GFP-tagging Interferes with Myosin Function and Sarcomere Assmebly in C. *elegans*

Michael Russell, Kia Skipper, and Ryan Littlefield

Department of Biology, UNIVERSITY OF SOUTH ALABAMA, Mobile, AL 36688

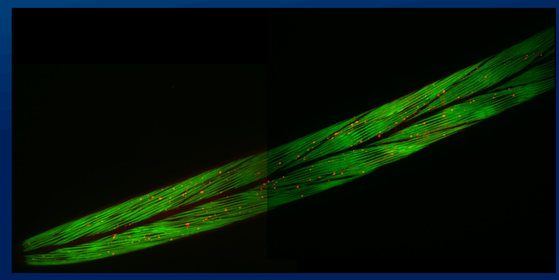

Abstract

In animals, myosin heavy chain (MHC) II motors undergo rapid attachment/detachment cycles on actin filaments to generate the mechanical forces and movement responsible for muscle and non-muscle contraction. To observe MHC II assembly into muscle thick filaments within an intact organism, we used CRISPR-based homologous repair to generate GFP-MyoB, an N-terminal fusion of GFP and unc-54, the major MHC II isoform in C. elegans body wall muscle (BWM). Remarkably, C. elegans strains homozygous for GFP-MyoB (GFP/GFP) have significant impairment in muscle sarcomere organization and function compared to either wildtype (+/+) or GFP-MyoB heterozygous (GFP/+) strains. To assess BWM function, organization, and assembly, we used swimming assays, confocal microscopy of live adults, and single plane illumination microscopy (SPIM) of developing embryos. In swimming assays, movement of GFP/GFP worms was reduced by ~50% compared to +/+ and GFP/+ worms. Within GFP/GFP adults, BWM thick filaments appeared as non-uniform clusters instead of broad, well-aligned oblique striations found in +/+ and GFP/+ adults. Defects in muscle function and structure appeared at initial myofibril assembly during embryogenesis. Surprisingly, while GFP/+ worms began twitching and moving within the egg, many GFP/GFP worms displayed a hypercontracted appearance with reduced twitching and moving. Our data suggest that GFP may sterically interfere with the efficient detachment of myosin motors from actin filaments and that this process is important for myofibril assembly, organization, and function in C. elegans.

Figure 1

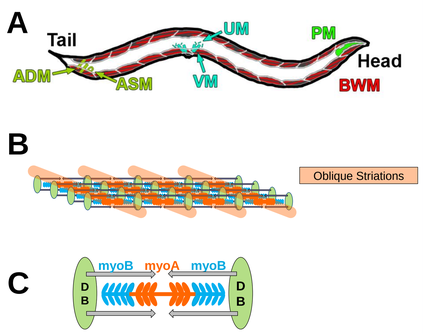

Figure 1. Myofilaments in *C. elegans* muscles
A) Diagram of *C. elegans* hermaphrodite muscle types include the pharynx muscles (PM) and body muscles, which include obliquely striated body wall muscle (BWM), vulval muscle (VM), uterine muscle (UM), anal depressor muscle (ADM), anal sphincter muscle (ASM). Males (not shown) have additional tail muscles. These muscles are composed of actin (thin) and myosin (thick) filaments that are organized into units (sarcomeres) which generate force. B) In BWM, thick filaments form oblique striations relative to the direction of contractile force. [2]. C) Within *C. elegans* body muscles, myoA (orange) and myoB (blue) myosin isoforms (encoded by *myo-3* and *unc-54*, respectively) co-assemble into 10 µm bipolar thick filaments [1]. Myosin motors domains (ovals) pull thin filaments (gray arrows) toward the center and transmit contractile force through dense bodies (DB, green) to the worm cuticle

Methods

Figure 2

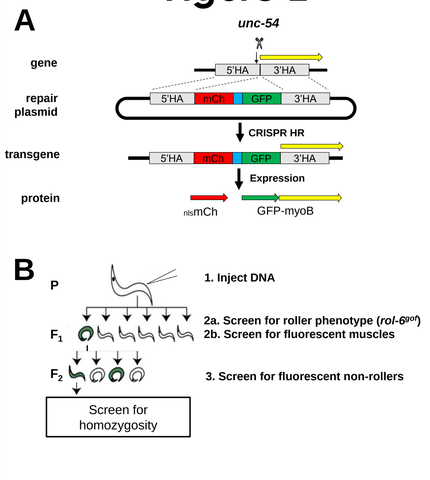

Figure 2. Design of *unc-54* transgenes using CRISPR-Cas9
A) The 5' end of the genomic *unc-54* locus was chosen to generate N-terminal fusion proteins using CRISPR-Cas9 homologous recombination (HR) [3,4]. The repair plasmids consist of 5' and 3' homology arms (HA), an insert containing an intercistronic region (blue) and sequences coding for mCherry (mCh) and green (GFP) fluorescent proteins. The transgenic *unc-54* gene is designed to express a GFP-myoB fusion (GFP-myoB). B) Transgenic worms were generated by injecting wildtype N2 worms (P) with DNA plasmids. Resulting progeny (F1) were screened for the phenotypic marker (*rol-6su1006*) and GFP expression. F2 non-rollers that expressed GFP were picked onto individual plates and screened for homozygosity.

Results

Figure 3

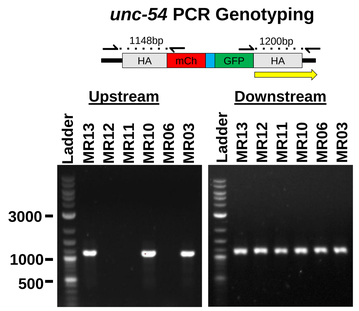

Figure 3. PCR genotyping of transgenic myosin worms
Agarose gel electrophoresis of *GFP-unc-54* (MR03, MR06, MR10, MR11, MR12, MR13) transgenic strains detecting the insert at the 5' (upstream) and 3' (downstream) ends of the target site. DNA standard (Ladder) sizes (bp, right of gel).

Figure 4

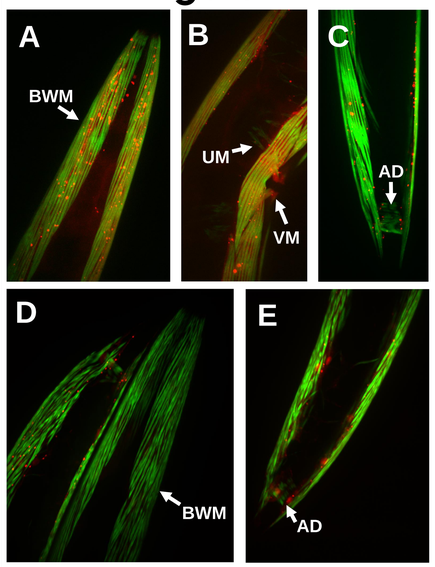

Figure 4. GFP-myoB assembles into thick filaments
GFP-MyoB (green) assembles into body muscle sarcomeres in heterozygous (A-C) and homozygous (D-E) adult worms. Co-expression of nls-mCherry (red) occurs within the same cells and localizes to the nuclei and some cytoplasmic aggregates. Heterozygotes have well-aligned sarcomeres. Homozygotes have more disrupted sarcomeres than heterozygotes. Body wall muscle (BWM); uterine muscle (UM), vulva muscle (VM), anal depressor muscle (AD).

Figure 5

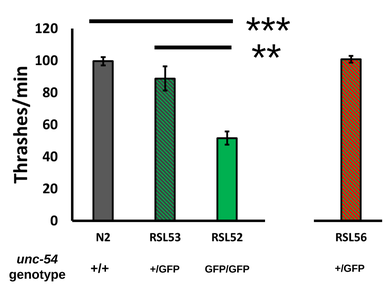

Figure 5. Homozygous GFP-unc-54 have impaired motility
Swimming assay (15 sec) was used to measure thrashing rates for young adult worms of four strains (N2, RSL53, RSL52, and RSL56). Average ± S. E. (n=10) for a representative experiment is shown. All strains were independently assayed three (A) or two (B) times. RSL52 thrashing rate was significantly different from N2 and RSL53 strains. P<0.001 (**), P<0.00001 (***). RSL52 and RSL53 were obtained from MR10 by outcrossing 5x with N2. RSL56 co-expresses mCherry-myoA and GFP-myoB.

Figure 6

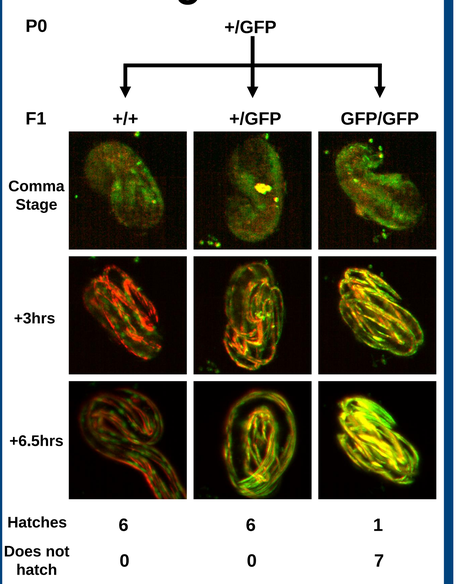

	+/+	+/GFP	GFP/GFP
Hatches	6	6	1
Does not hatch	0	0	7

Figure 6. Sarcomere assembly during worm development is impaired in embryos homozygous for GFP-MyoB
Progeny of RSL56 heterozygotes were imaged using Selective Plane Illumination Microscopy (SPIM) to compare sarcomere assembly and hatching. Progeny were categorized according to *unc-54* genotype based on GFP intensity. Most progeny homozygous for GFP-MyoB become unable to move in the eggshell and fail to hatch. All images are maximum Z projections and all genotypes are identically displayed.

Figure 7

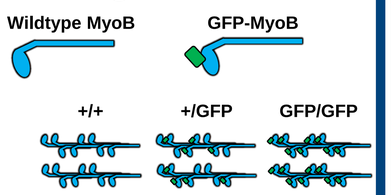

	+/+	+/GFP	GFP/GFP
Contraction	Normal	Normal	Normal
Assembly	Normal	Normal	Normal
Relaxation	Normal	Normal	Impaired
Alignment	Normal	Normal	Impaired

Figure 7. Working model for MyoB impairment by GFP-tagging
GFP-MyoB is able to assemble into thick filaments with wildtype or GFP-MyoB and generate contractile forces. Steric inhibition of GFP is hypothesized to reduce the myosin head detachment rate of from the actin filament and impair myofibril relaxation. Impaired relaxation may lead to misalignment of the thick filaments and impairment of muscle function over time.

Conclusions

- The *C. elegans* muscle myosin heavy chain gene *unc-54* was fluorescently tagged by CRISPR-Cas9 gene editing using a co-CRISPR strategy (Figure 2).
- Six independent transgenic strains were isolated. Three strains (MR3, MR10, and MR13) have the expected insert sizes at the *unc-54* locus (Figure 3) and express both mCh and GFP-myoB (Figure 4).
- The fluorescent tags in heterozygote animals are well-tolerated during muscle assembly and appear to have minimal impact on contractile function.
- Heterozygotes are fully motile and BWM striations are well-aligned.
- GFP-MyoB localizes to wide double striations (doublets) in BWM and a broad, wide doublet in AD (Figure 4), consistent with its position in the middle of thick filaments (Figure 1). [1]
- The GFP tag on MyoB result in a recessive motility defect. Homozygote strains lead to reduced motility (Figure 5).
- Initial sarcomere assembly and embyro elongation occur normally during development for GFP-MyoB homozygotes, but most fail to hatch because of reduced movement in the egg.
- We hypothesize that the muscle defects we observe is due to steric blocking of myosin heads by the GFP tag and abnormal muscle relaxation.

Literature Cited

[1] Miller, D. M. III, Ortiz, I., Berliner, G. C., and H. F. Epstein, 1983. "Differential localization of two myosins within nematode thick filaments". Cell, vol. 34(2).

[2] Moerman, D. G. and Williams, B. D. Sarcomere assembly in C. elegans muscle (January 16, 2006), WormBook, ed. The C. elegans Research Community, WormBook, doi/10.1895/wormbook.1.81.1, http://www.wormbook.org.

[3] D. J. Dickenson, J. D. Ward, D. J. Reiner, B. Goldstein, "Engineering the *Caenorhabditis elegans* genome using Cas9-triggered homologous recombination," Nature Methods, vol. 10 pp. 1028-1034, 2013.

[4] J. A. Arribere, R. T. Bell, B. X. Fu, K. L. Artiles, P. S. Hartman, A. Z. Fire, "Efficient marker-free recovery of custom genetic modification with CRISPR/Cas9 in *Caenorhabditis elegans*," Genetics, vol. 198 pp. 837-846, 2014

Acknowledgements

We thank Drs. Sherman, Kroetz, and Ni Chadhain for the use of their lab equipment, and the other members of the Littlefield Lab for their support. We thank the imaging core at USA medical school (NIH Grant:1S10 OD02149-01) for the use of the Andor spinning disk confocal microscope. We thank Drs. Hari Shroff and Ryan Christensen for the use of and training on the dual-inverted selective plane illumination microscope (diSPIM) at the High Resolution Optical Imaging Lab (NIBIB, NIH). The N2 strain was provided by the CGC, which is funded by NIH Office of Research Infrastructure Programs (P40 OD010440).This research was supported by a 2016 USA Faculty Development Grant, AL EPSCoR Grant, and the NSF EPSCoR Grant to RSL.